Research paper

Determining the end of primary consolidation parameters based on settlement and excess pore water pressure

Bartłomiej Szczepan Olek[1]

Abstract: The multiple-stage loading with reloading at EOP tests were carried out on two high-plasticity remoulded clays. One percentage of the initial value of an excess pore water pressure has been adopted as a reference for the end of the primary consolidation criterion. Based on the measurements of the settlement with time, six methods were used for determining the EOP parameters. For all studied consolidation curves, the primary consolidation time determined by settlement data was always smaller than those specified by dissipation data. All analysed cases have observed the lack of complete dissipation at the primary consolidation time determined by settlement data. The magnitude of remaining pore pressure at the primary consolidation time determined by various methods and the degree of additional settlement induced by remaining pore pressure at the primary consolidation time indicate an underestimation of EOP parameters when the interpretation of the test is based only on the analysis of sample settlement. Based on the average degree of consolidation imposed by the excess pore water pressure dissipation at primary consolidation time, the most similar time values at EOP to that determined using the excess pore water pressure dissipation criterion were obtained using the SRS, Casagrande and Slope methods.

Keywords: clay, consolidation, dissipation, end of primary, excess pore water pressure

[1]PhD., Eng., Cracow University of Technology, Faculty of Civil Engineering, Warszawska 24, 31-155 Cracow, Poland, e-mail: bartlomiej.olek@pk.edu.pl, ORCID: 0000-0002-7830-5635

1. Introduction

The deformation of fine-grained soils subjected to a change in total vertical stress results from primary and secondary consolidation [1, 2]. Primary consolidation occurs during the dissipation of excess water pressure in the pores, i.e. during the increase in effective stress. Secondary consolidation takes place under constant effective stress after the stress transfer from pore water to the soil framework. This additional compression in relation to the primary compression depends on time and the visco-plastic properties of the soil skeleton. The dominant process during secondary consolidation is creep, defined as a process in which soil deformation will occur as a function of time and the creep rate is controlled by viscous resistance [3]. From a practical point of view, settlements of thick in-situ soil layers are generally predicted based on extrapolation of experimental results originating from thin laboratory specimens. The model law of consolidation is used for this purpose, i.e., the "H^2 rule", which gives a simple method for determining the degree of consolidation in a layer if the simplifying assumption is made that the settlement recorded in the consolidation test is purely due to primary consolidation. This approach is based on the classic theory of consolidation [4]. Considering a given soil type and identical drainage conditions, the theory relates the EOP consolidation time (t_{thick}) of a thick soil layer (H_{thick}) to the EOP consolidation time (t_{thin}) of a thin soil layer (H_{thin}) based on the square ratio of the two thicknesses:

$$(1.1) \qquad \frac{t_{\text{thick}}}{t_{\text{thin}}} = \left(\frac{H_{\text{thick}}}{H_{\text{thin}}}\right)^2 \quad \text{or} \quad \frac{t_{\text{in–situ}}}{t_{\text{lab}}} = \left(\frac{H_{\text{in–situ}}}{H_{\text{lab}}}\right)^2$$

In other words, following Smith [5], if two layers of the same fine-grained soil with different drainage path lengths, H_1 and H_2, are acted upon by the same pressure increase and reach the same degree of consolidation in times t_1 and t_2, respectively, then theoretically their coefficients of consolidation (c_v) must be equal as must their time factors, T_1 and T_2:

$$(1.2) \qquad T_1 = \frac{c_{v1}t_1}{H_1^2}; \quad T_2 = \frac{c_{v2}t_2}{H_2^2}$$

The distance of the longest vertical path water takes to exit the soil is called the length of the drainage path. The relations 1.1 and 1.2 are valid for an assumption that disregards creep during primary consolidation. However, Ladd et al. [6] imposed two extreme hypotheses on whether or not creep acts as a separate phenomenon, during excess pore pressure dissipation. Hypothesis A assumes that the relationship between effective stress and strain is independent of the duration of primary consolidation [7]. In the case of hypothesis B, the final deformation at the end of primary consolidation (EOP) is determined by the duration of this stage [8]. It, therefore, depends on the thickness of the soil layer. Hence, the occurrence of creep during the primary consolidation implies that the consolidation process is delayed, resulting in longer EOP times [9].

Using hypothesis A for resolving practical problems demands data from laboratory tests, preferably tests with the pore water pressure measurements. Observing the evolution of pore pressure during the test directly allows us to determine the EOP state. However, this type of data is not always available, and the time or strain at EOP is determined based on the course of deformation. Currently, several methods are available for determining EOP from

the time-settlement curve. The main goal of this work is to check which methods provide the most similar results to those derived from pore pressure observations. For this purpose, special multiple-stage loading with reloading at the EOP tests $(MSL)_{EOP}$ were carried out, in which the duration of particular load steps depended on the dissipation time. The dissipation time and final values of excess pore water pressure resulted strictly from the EOP criterion. Moreover, with the results of the $(MSL)_{EOP}$ tests, the conditions at EOP were analysed in terms of the degree of additional settlement induced by the remaining pore pressures at EOP determined by strains and the magnitude of remaining pore water pressure at EOP established by time-settlement curve.

2. Materials and methods

2.1. Soil material used in the study

The investigated soil was a Polish Miocene clay called Krakowiec clay. It was formed in the Carpathian Foredeep due to the early-Baden marine transgression [10]. For the purposes of the study, the soils were collected from two locations in Poland and designated as follows: Krakowiec Clay 1 (Zesławice) and Krakowiec Clay 2 (Chmielów). The geotechnical properties of the clay formation were found to be variable in terms of Atterberg limits, consistency and mineralogical composition having various proportions of clay, silt and sand fractions [11]. The detailed geological and geotechnical characterisation of the intact, remoulded or reconstituted Krakowiec clay can be found in past studies [12–17]. Thus, Table 1 presents the most relevant index properties of the studied soils. Two clays were remoulded at water contents close to their liquid limits (LL). For each MSL_{EOP} test, the grain size distribution (percentages of sand, silt and clay fractions), specific gravity (G_s), and Atterberg limits, i.e. plastic limit (PL) and liquid limit (LL), were determined according to ISO standards. Based on the plasticity index $PI = LL − PL$ and Casagrande's classification chart for the fine-grained soils, the tested soils were high-plasticity clays.

Table 1. Basic index properties of the soils utilised in the present study

Sample	G_s (–)	Grain-size distribution			Atterberg limits		
		Sand (%)	Silt (%)	Clay (%)	PL (%)	LL (%)	PI (%)
Clay 1	2.66	1	22	77	30	86	56
Clay 2	2.72	2	53	45	24	65	41

2.2. Consolidation tests

To describe the conditions at EOP consolidation, the consolidation tests using the Rowe cell testing system [18] have been utilised. The key components of the set-up used consisted of a VJT0640 Rowe cell connected to the Automatic pressure controller (APC) and the data acquisition system, as shown in Figure 1.
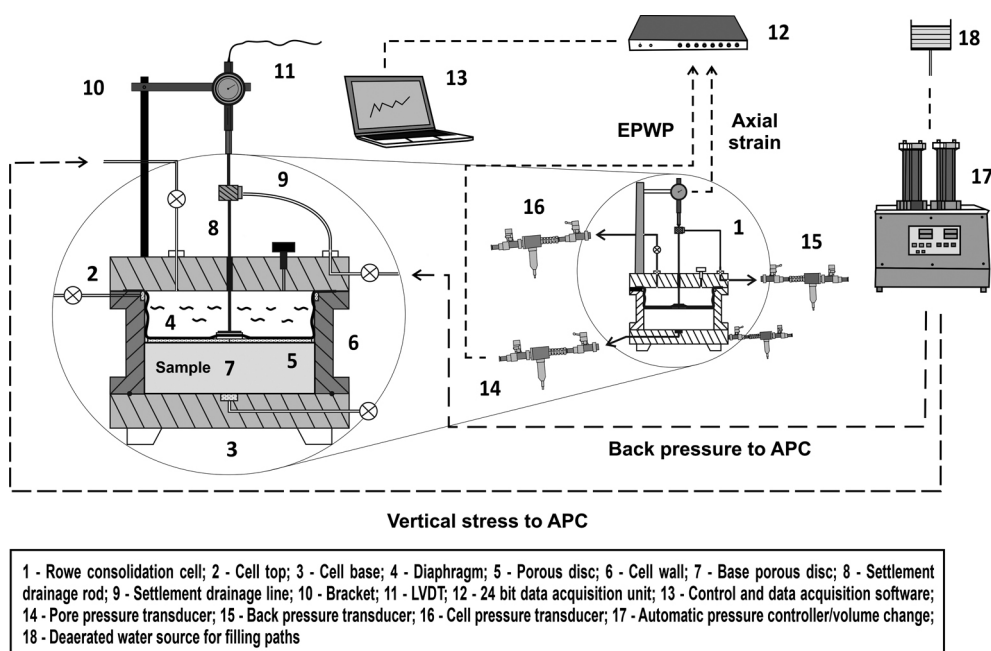
1 - Rowe consolidation cell; 2 - Cell top; 3 - Cell base; 4 - Diaphragm; 5 - Porous disc; 6 - Cell wall; 7 - Base porous disc; 8 - Settlement drainage rod; 9 - Settlement drainage line; 10 - Bracket; 11 - LVDT; 12 - 24 bit data acquisition unit; 13 - Control and data acquisition software; 14 - Pore pressure transducer; 15 - Back pressure transducer; 16 - Cell pressure transducer; 17 - Automatic pressure controller/volume change; 18 - Deaerated water source for filling paths

Fig. 1. Schematic of the Rowe cell consolidation set-up

The settlement (vertical displacement) and excess pore water pressure dissipation data employed in the study were measured during the $(MSL)_{EOP}$ tests under the guidance given by Head [19]. The specimens were consolidated under the given load increment in the test until the adopted EOP criterion was fulfilled. Different criteria for defining EOP based on excess pore water pressure have been suggested in the technical literature. As a rule, these criteria are based on initial (u_0) and final excess pore water pressure (u_f). Choi [20] depended on the possibility of applying the next load step after reaching u_f close to zero. In turn, Mesri and Choi [7] adopted EOP as $u_f = 2\% u_0$. Consecutively, 1% of u_0 was assumed by Imai and Tang [21] and Mesri [22], while the criterion based on u_f was approximately equal to 1 kPa by Feng [23], Kabbaj et al. [24] and Kim and Leroueil [25]. Konovalov and Bezvolev [26] and Watabe et al. [27] adopted the criterion of 5% u_0 and 2% u_0, respectively. The study presented herein measured the pore water pressure at the sample's lower end using the VJT/0260-AP pore pressure transducer. The transducer used has an accuracy of pressure measurement of 0.1% full range, resolution of 0.1 kPa measured values and resolution of volume measurement of 0.5 mm³. The EOP criterion was established based on restrictive criteria, i.e. initial and final excess pore water pressure, $u_f = 1\% u_0$. In this way, the duration of each load increment depended on the time to complete the dissipation of the excess pore water pressure and this time was determined as time at EOP. The consolidation tests were performed on specimens placed in the stainless steel cell with a diameter of 75.5 mm. They were loaded hydraulically by the water pressure acting on a rubber diaphragm. The drainage was allowed vertically using the previous top and impervious bottom surfaces (PTIB). The porous

disc was boiled with de-aired water before being placed into the cell. On the other hand, the internal sides of the cell were lubricated with silicone grease to minimise side friction. The testing procedure consisted of two stages, i.e. saturation and consolidation. The ramp method [28] was used to ensure the sufficient saturation of the samples. The cell and back pressure were ramped, and the B-check was performed regularly to examine whether the required B-value (i.e. Skempton's pore pressure coefficient B) was reached. Each sample was assumed to be saturated if the B-value was higher than 0.98. Then, the consolidation was initiated by opening the external pressure valve while the back-pressure pressure valve was closed. Thus, the pore pressure was increased and reached a certain level equal to the load increment, and the sample did not settle. After the pore pressure stabilised, the opening of the back-pressure valve enabled pore pressure to dissipate with the sample deformation simultaneously. For the tests with a uniform stress distribution, the following loading scheme was adopted: $12.5 \rightarrow 25\,\text{kPa} \rightarrow 50\,\text{kPa} \rightarrow 100\,\text{kPa} \rightarrow 200\,\text{kPa} \rightarrow 400\,\text{kPa} \rightarrow 800\,\text{kPa}$. In this connection, the load increment ratio (LIR) was 1.0. The results indicate that the soils were clays of high plasticity.

2.3. Determining EOP parameters

Over the past decades, various curve-fitting methods for consolidation analysis have been developed. Some gained attention and recognition, while others were rarely used. The most popular approaches for evaluating EOP parameters include the graphical interpretation of the time-settlement curve or its different modes. This paper focuses on six methods, namely: Logarithm of time (Casagrande method) [29], Square root of time (Taylor method) [30], $\delta - t/\delta$ (Sridharan method) [31], Rectangular hyperbola (Hyperbolic method) [32, 33], Settlement-rate settlement (SRS method) [34], and Slope method [35].

The Logarithm of time fitting method was developed based on the observation that the plot of average degree of consolidation (U_v) versus time factor (T_v) has three distinct portions: an initial parabolic-shaped portion, a linear middle portion and a final portion asymptotic to the horizontal (see Fig. 2a). The middle and last portions of the time-settlement relationship are used for determining EOP. The method requires drawing a straight line passing through the final points, which exhibit a linear trend with constant inclination and tangent to the steepest part of the curve. The intersection formed by the last straight line was produced backwards, and the tangent to the curve at the point of inflection represents 100% of the primary consolidation, e.g., time and settlement at EOP (see Fig. 2b).

The square root of time method utilises the initial linear portion of the settlement-time curve to establish 90% consolidation. For determining EOP consolidation, a straight line is drawn through the 0% compression ordinate so that the abscissa of this line is 1.153 times the abscissa of the initial linear segment through the data (see Fig. 2c). The factor of 1.153 is the ratio of the secant slope, at 50% consolidation, to the secant slope, at 90% consolidation. The time corresponding to the intersection of the second line with the curve represents 90% primary consolidation. For interpretation purposes, a third point taken at $U_v = 90\%$ estimates the EOP settlement. The method also allows us to obtain the point where the primary consolidation is assumed to be complete (i.e. $U_v = 100\%$).
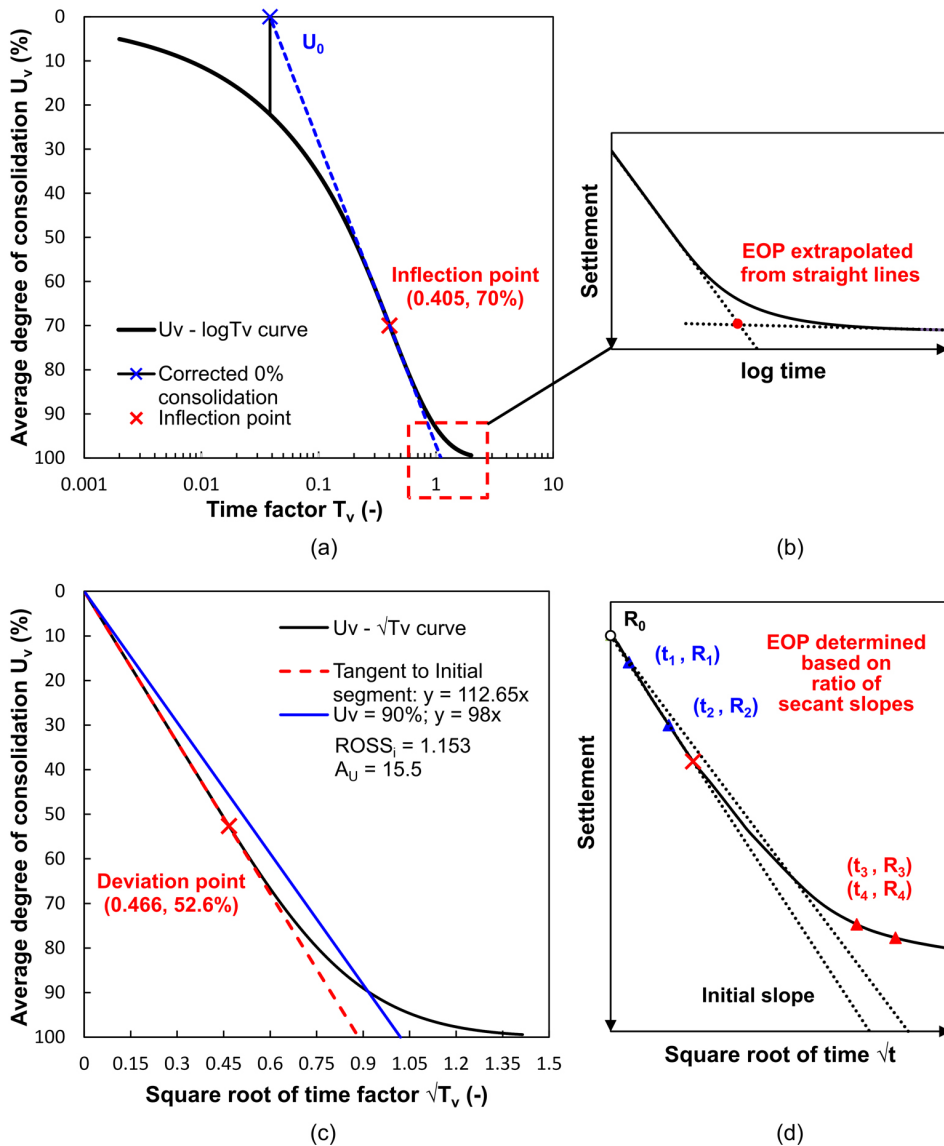
Fig. 2. Principles for determining EOP parameters; (a) theoretical plot used in the Casagrande method, (b) schematic of experimental procedure, (c) theoretical plot used in the Taylor, Slope and Modified slope methods, (d) schematic of experimental procedures (Note: A_U is the percentage increase in the abscissa for Taylor method)

A modification of the Taylor method is the Slope method [35]. The method is based on a fitting procedure in which the slope of the initial linear segment of the $\delta - \sqrt{t}$ curve is fitted to the corresponding slope of the $U_v - \sqrt{T_v}$ relationship, which is constant and is equal to 1.128.

The compression (δ_e) at which the $\delta - \sqrt{t}$ curve deviates from the initial linear portion was used for estimating EOP consolidation (see Fig. 2d). The procedure for determining the EOP consolidation incorporated in the Slope method was modified by the same author [36] and was based on a unique relationship between the ratio of the secant slopes (ROSS$_i$) of $\delta - \sqrt{t}$ curve at 50% consolidation to the secant slope at any time arbitrarily selected U_v beyond the deviation point. The modified slope method requires selecting at least four compression-time data points for establishing EOP (see Fig. 2d).

It should be remembered that selecting points that relate to significant compression in the later stages of consolidation may lead to unrealistically large consolidation EOP values. Hence, the method is prone to the interpreter's judgement.

Sridharan and Prakash [31] used theoretical U_v versus T_v/U_v plot to improve determining EOP consolidation. The procedure of $\delta - t/\delta$ method is based on the initial straight line portion as in the U_v versus $\sqrt{T_v}$ plot. The results from the $\delta - t/\delta$ curve compare well with the results by the Taylor method. Because of the flatter slope of 1/1.33 ($\delta - t/\delta$ curve) against 1/1.15 ($\delta - \sqrt{t}$ curve), the 90% consolidation point estimation is more accurate. Based on experimental observations, it can be concluded that EOP settlements determined using the $\delta - t/\delta$ method are comparable to those specified on the basis of the square root of time plot.

Sridharan and co-workers [32] have made another attempt to analyse consolidation test results. They proposed the rectangular hyperbola method (Hyperbolic method) to describe the relationship between T_v and U_v as a rectangular hyperbola (see Fig. 3a, b). The EOP settlement, in this case, is predicted using the non-dimensional slope of the t/δ versus t plot, i.e. l/mH_i. By comparing the theoretical T_v/U_v versus T_v and experimental t/δ versus t curves, an analytical expression for EOP settlement has been proposed [33]:

$$(2.1) \qquad\qquad \delta_{100}/H_i = \frac{0.859}{mH_i}$$

Note that, determining EOP consolidation in this method does not require knowledge of the initial compression. The authors pointed out that the hyperbolic approach significantly improves the estimation of the 90% primary consolidation point compared to the Taylor method because the slope of the $U_v - T_v/U_v$ curve decreases more rapidly than that of the $U_v - \sqrt{T_v}$ curve [32].

The Settlement rate settlement method involves a fitting procedure in which the slope of the linear section of the experimental $d\delta/dt - \delta$ curve is fitted to the corresponding slope of the linear section of the theoretical $dU_v/dT_v - U_v$ relationship at the average degree of consolidation $U_v \geq 52.6\%$ (see Fig. 3c,d) [34]. The settlement at EOP is deemed by extrapolating the settlement data obtained from the primary consolidation stage so that the extension of the linear section of the experimental curve intersects the settlement axis when the settlement rate is equal to 0. Accordingly, the EOP settlement is computed as a ratio of the intercept to the slope of the linear section of the curve. Al-Zoubi [37] compared EOP settlements determined by the SRS method with those obtained from the Casagrande method. The results showed that the EOP settlement values were quite similar, though Casagrande values were slightly higher in general.
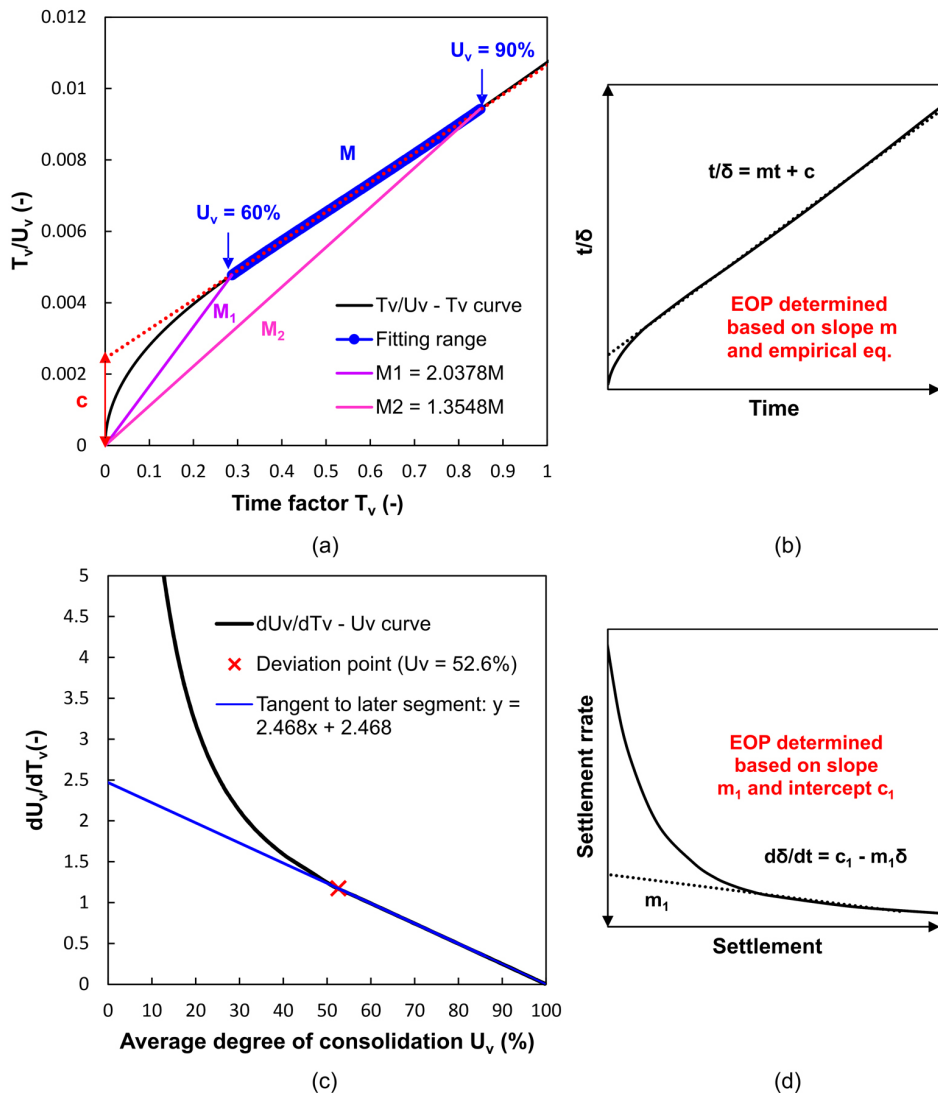
Fig. 3. Principles for determining EOP parameters; (a) theoretical plot used in the Hyperbolic method; (b) schematic of experimental procedure, (c) theoretical plot used in the Settlement rate settlement (SRS) method, (d) schematic of experimental procedure

3. Results and discussion

3.1. General consolidation behaviour

Conducted consolidation tests allowed simultaneous measurements of vertical deformation and pore water pressure at the base of the sample (u_b). Before proceeding with an analysis,

the pore pressure data has been converted into the degree of dissipation (U_{ub}) for assessing consolidation behaviour. The expression for degree of dissipation is as follows:

$$(3.1) \qquad U_{ub} = \left(\frac{u_0 - u_i}{u_0} \right) \times 100\%$$

where: u_0 – excess pore water pressure at the initial stage of consolidation, u_i – excess pore water pressure at time t.

That way, the dissipation progress was expressed as a percentage acting as a global measure of the process. The time-strain and time-degree of dissipation curves obtained from tests are shown in Fig. 4.
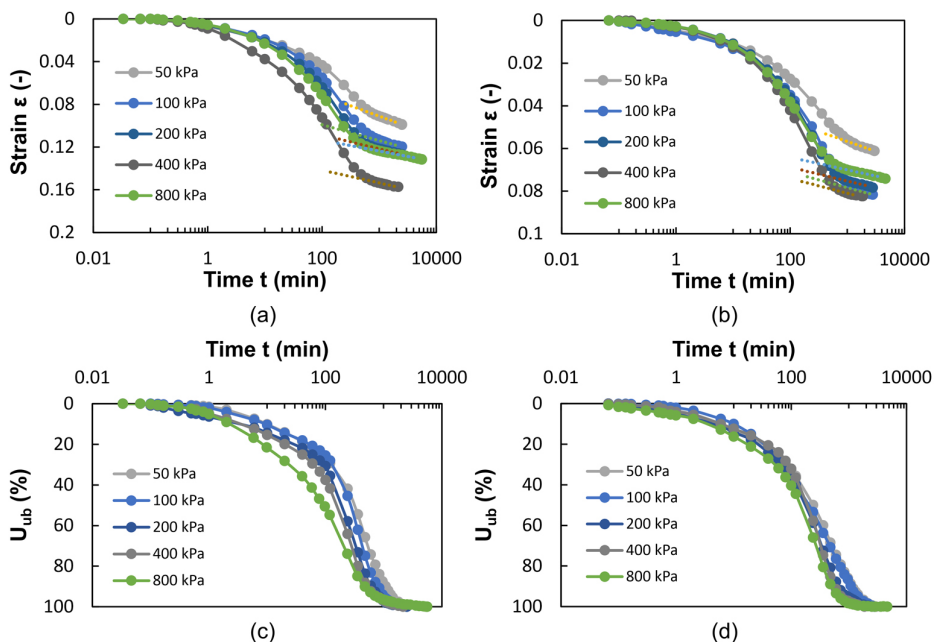
Fig. 4. Consolidation behaviour of soils; (a) vertical strain vs time curves (Clay 1), (b) vertical strain vs time curves (Clay 2), (c) degree of dissipation U_{ub} vs time curves (Clay 1), (d) degree of dissipation U_{ub} vs time curves (Clay 2)

In the semi-logarithmic plot, all time-strain curves exhibit a typical S-shaped course with a clear linear section of the secondary consolidation (marked by dotted lines). Note that the changes in strain presented in Fig. 4a and b refer to the engineering strain, defined as the change in length divided by the initial length for the considered load step, i.e. $\varepsilon = \Delta H / H_0$. The coefficient of secondary consolidation ($c_{\alpha\varepsilon}$) has been calculated for each curve. It is interesting to note that $c_{\alpha\varepsilon}$ changed with vertical effective stress following the power rule.

As can be seen from Fig. 4, the strain rates have increased with the increase of effective vertical stress up to $\sigma'_v = 400$ kPa for the two clays. The dissipation rates systematically increased with effective vertical stress, as illustrated by the shift to the left location of curves.

Table 2 presents parameters describing initial and final conditions for particular load increments. In the experiments, the loads were instantaneously transferred to the sample, and the generated excess pore water pressure reached its maximum value within a few seconds. Thus, the phenomenon of time delay, i.e. time lag, practically did not occur. The $u_b(max)$ values were very close to the load increments. The calculated $C_{IL} = \Delta u / \Delta \sigma_v'$ values were close to 0.99, indicating that the theoretical assumption of complete load transfer to the liquid phase at the start of the test was met. Obtained data support the concept of $C_{IL} = 1$ at $t = 0$ for saturated soft clays [38, 39].

Table 2. Conditions at initial and final stages of the Rowe cell with reloading at EOP tests

σ_v'	$\Delta\sigma_v'$	$u_b(max)$ (kPa)	$C_{IL}(-)$	u_{bk} (kPa)	u_0 (%)	t_{pu} (min)
Clay 1						
50	25	24.99	1.000	0.68	2.73	2499
100	50	49.99	1.000	1.09	2.19	2499
200	100	99.79	0.998	1.07	1.07	2499
400	200	199.12	0.996	1.88	0.95	2160
800	400	398.14	0.995	3.98	1.00	5566
Clay 2						
50	25	24.95	0.998	0.88	3.53	2990
100	50	49.56	0.991	1.08	2.18	2788
200	100	99.62	0.996	1.15	1.16	2790
400	200	198.95	0.995	2.00	1.01	1879
800	400	397.86	0.995	4.08	1.03	3830

A closer examination of pore pressure dissipation curves showed incomplete pore pressure dissipation to zero at the end of each test step, mainly due to the type of test carried out (MSL$_{EOP}$) and the adopted EOP criterion. Nevertheless, Zeng et al. [40] and Zeng et al. [41] also reported the lack of complete pore pressure dissipation in laboratory consolidation tests. The ratio of u_{bk} to the $u_{b(max)}$, i.e. % u_0 for the first two load increments, was the highest and comprised between 2.1% and 3.5%. The ratio values for the remaining load increments were close to or lower than 1%.

3.2. Conditions at EOP consolidation

Based on the measurements of the settlement and excess pore water pressure with time, seven methods were used for determining the EOP parameters. Considering the pore water pressure records, the time to archive the adopted EOP criterion was identified as time at EOP, i.e. t_{pu}. Applying the six methods utilizing settlement records for all considered load increments revealed that the primary consolidation time t_p was always smaller than t_{pu}. It has also been observed that there is a lack of complete dissipation at the t_p. Figure 5 illustrates the changes

in the ratios of t_p/t_{pu} with σ'_v for two clays. In the case of Clay 1, the ratios of t_p/t_{pu} showed a clear decreasing trend with the increase in σ'_v. The lowest ratio values were obtained for the Sridharan, Taylor and Hyperbolic methods and the highest for the SRS and Slope methods. For Clay 2, the ratio values increased and then decreased with increasing σ'_v. Considering individual methods, similarly to Clay 1, the lowest ratio values are related to the Sridharan, Taylor, and Hyperbolic methods. Significant differences in changes in the ratios of t_p/t_{pu} with the effective vertical stress for the two soils result mainly from the different shapes of the middle and end sections of the curves used to determine the time at EOP with a given method.
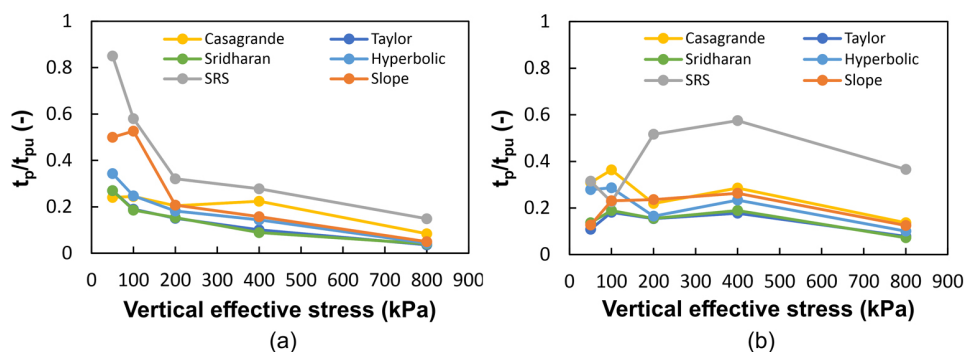
Fig. 5. Ratios of t_p/t_{pu} comparing EOP times determined by the methods based on settlement records with this utilised pore water pressure dissipation; (a) Clay 1, (b) Clay 2

The ratio of t_p/t_{pu} values indicated that there exists a magnitude of remaining pore pressure at the t_p determined by the given method based on settlement data, denoted as $D_{utp} = (u_{btp}/\sigma'_v)\cdot 100\%$. The u_{btp} is the base pore water pressure measured at EOP consolidation time using settlement data. Figure 6a, b presents relationships between D_{utp} and σ'_v. The values of D_{utp} calculated using u_{btp} from the Casagrande method exponentially decreased with the increase in σ'_v for both clays. Determining EOP by the Casagrande method strongly depends on the shape of the latter section of the settlement-time curve (i.e. secondary consolidation tail) and, consequently, the $c_{\alpha\varepsilon}$ value. Therefore, the D_{utp} calculated on the basis of this method can be related to creep susceptibility, expressed in terms of $c_{\alpha\varepsilon}$ (see Fig. 6c). As seen, excellent linear relationships have been obtained with high values of R^2. When examining rest methods, a similar pattern of D_{utp} against σ'_v has been observed using Slope and SRS methods for Clay 2. Considering results for Clay 1, in most cases, the magnitude of remaining pore pressure at the t_p increased with the increase in σ'_v, except for load increment from 400 kPa to 800 kPa, when D_{utp} was calculated based on Taylor, Sridharan and Slope methods. Different behaviour has been observed for Clay 2. For Taylor, Sridharan and SRS methods, D_{utp} decreased up to 200 kPa and then increased or stabilised. In turn, D_{utp} determined by the Hyperbolic method to a minor extent varied with σ'_v.

It should be noted that the Taylor, Sridharan and Slope methods depend on the slope of the consolidation curve's initial part. In contrast, the Hyperbolic method depends on the middle part and the SRS method on the middle-latter. This explains the position of the curves
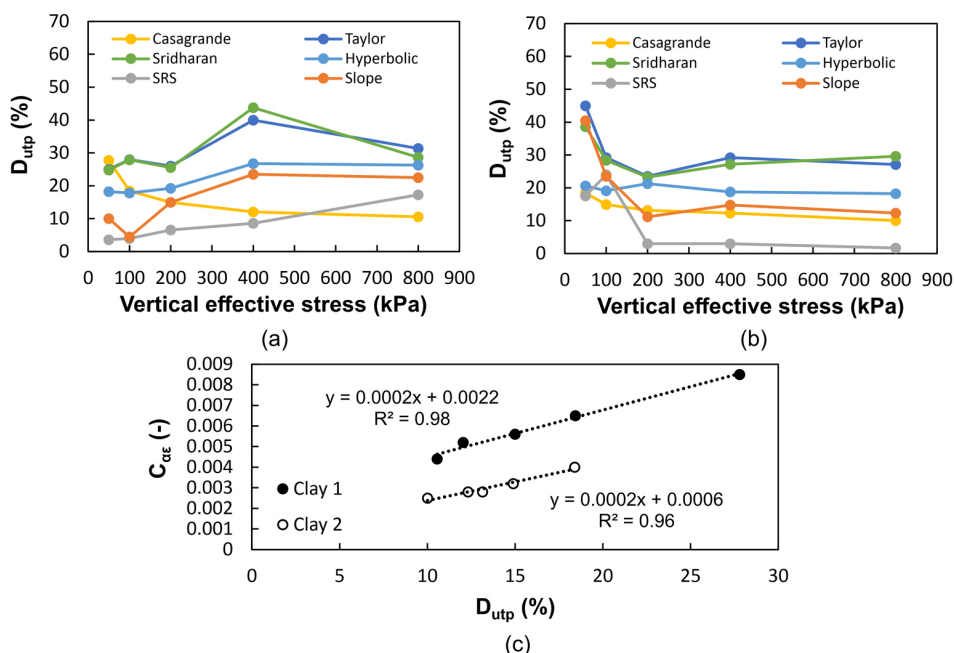
Fig. 6. Magnitude of remaining pore pressure D_{utp} determined by various methods; (a) Clay 1, (b) Clay 2, (c) relationships between $c_{\alpha\varepsilon}$ and D_{utp} based on the Casagrande method

relative to each other on the plots. The highest positions taken curves related to the Taylor and Sridharan methods, slightly lower for the Hyperbolic and Slope methods and then for the Casagrande and SRS methods. In this connection, there is a clear decreasing trend in the value of D_{utp} in the following order: Taylor and Sridharan methods mostly within a range of 25% to 45%; Hyperbolic method mostly within a range of 18% to 27%; Slope method mostly within a range of 4% to 40%; Casagrande method mostly within a range of 10% to 28%; SRS method mostly within a range of 3 to 17%. The wide range obtained for the Slope method was due to the extreme D_{utp} value of 40.5% calculated for a load of 50 kPa (Clay 2), with the rest of the values much lower for the considered soil.

Knowing the magnitudes of remaining pore water pressure at t_p, the degree of additional settlement induced by remaining pore pressure at the t_p determined by the given method has been calculated. Necessary data needed to figure this parameter was the settlement under the step load increment $\Delta\sigma'_v$ at the EOP consolidation time determined based on excess pore water pressure (Δs_{tpu}) and the settlement under the step load increment $\Delta\sigma'_v$ at the EOP consolidation time determined based on settlement data (Δs_{tp}). Figure 7a, b shows the changes in D_{stp} values with vertical effective stress. As can be seen, for Clay 1, considering the Casagrande method, the D_{stp} decreased, and around $\sigma'_v = 400$ kPa started to increase. In contrast, for other methods, D_{stp} increased with σ'_v, except for $\sigma'_v = 800$ kPa, when D_{stp} were stabilised. In the case of Clay 2, predominantly for almost all relationships, D_{stp} first decreased up to $\sigma'_v = 200$ kPa or $\sigma'_v = 400$ kPa and then started to increase. Similarly to
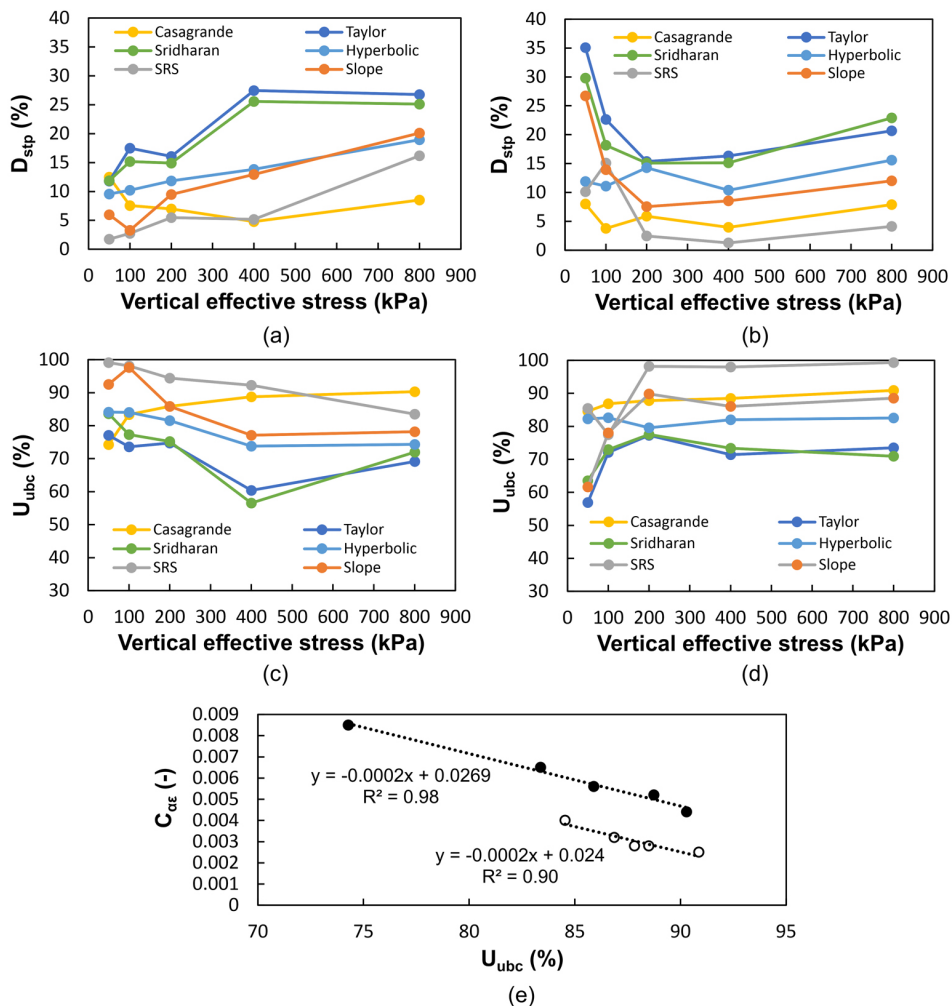
Fig. 7. Soil behaviour at EOP consolidation; (a) D_{stp} versus σ'_v for Clay 1, (b) D_{stp} versus σ'_v for Clay 2, (c) U_{ubc} versus σ'_v for Clay 1, (d) U_{ubc} versus σ'_v for Clay 2, (e) relationships between $c_{\alpha\varepsilon}$ and U_{ubc}

D_{utp}, depending on the method used, D_{stp} values were distributed within the following ranges: Taylor method 11.8–27.5%; Sridharan method 11.9–29.8%; Hyperbolic method 10–19%; Slope method 3.2–26.7%; Casagrande method 4–12.5%; SRS method 1.8–16.2%.

The last stage of the analysis consisted of determining the average degree of consolidation imposed by the excess pore water pressure dissipation at $t_p(U_{ubc})$. This parameter indicates precisely the percentage of dissipation of excess pore water pressure, i.e. the advancement of the consolidation process for time and settlement at EOP determined by a given method. It can, therefore, be concluded that the value of $100 - U_{ubc}$ corresponds to the D_{utp} value with the difference that U_{ubc} depends on the initial and final value of the recorded excess pore water pressure, whereas D_{utp} refers to the total increase in the vertical effective stress. As seen

from Fig. 7c, d, the $U_{ubc} - \sigma'_v$ curves are inversely positioned on the graph in relation to the $D_{utp} - \sigma'_v$ curves (see Fig. 6a, b). Based on the relationships between U_{ubc} and σ'_v, the most similar time values at EOP to that determined using the excess pore water pressure dissipation criterion were obtained using the SRS, Casagrande and Slope methods.

The remaining techniques, i.e. Hyperbolic, Sridharan and Taylor, indicated much shorter EOP times and thus much lower settlement at EOP or deformation at EOP and higher values of undissipated excess pore water pressure. The U_{ubc} values were also compared to the slope of the final section of the consolidation curve expressed by $C_{\alpha\varepsilon}$. Figure 7c shows linear relationships for the two clays tested. As can be seen, the higher the strain rate in the secondary consolidation phase, the higher the U_{ubc} value. This proves the retarding effect of creep on the dissipation of pore pressure for the advanced stage of consolidation, and on the other hand, it may explain the discrepancies between experimental observations and the theoretical solution resulting from Terzaghi's theory, which only takes into account the filtration aspect of the consolidation process.

4. Conclusions

The consolidation behaviour and conditions at EOP consolidation of two high-plasticity clays were evaluated using a Barden-Rowe-type consolidometer. One per cent of the initial value of measured excess pore water pressure was used as the end of the primary consolidation criterion. Six methods for determining time and settlement (deformation) at the end of primary consolidation were analysed based on settlement measurements over time. For all the analysed consolidation curves, the primary consolidation time determined based on the settlement records was always smaller than the time specified by an excess pore water pressure. A lack of complete dissipation at the end of primary consolidation was observed in all analysed cases, as determined by the settlement curve. This phenomenon indicated a magnitude of remaining pore pressure at the primary consolidation time determined by the settlement data. The D_{utp} and D_{stp} parameters were used to express this observation numerically. The results showed an underestimation of EOP parameters when the test interpretation is based solely on the sample's vertical deformation analysis. The highest t_p/t_{pu} ratio values were calculated for the lowest load values. A clear upward trend in the ratio values was observed in the following order: Taylor's method, mainly in the range from 0.04 to 0.27 – Sridharan's method, mostly in the range from 0.04 to 0.27 – Rectangular Hyperbola method, mainly in the range from 0.04 to 0.34 – Casagrande method usually in the range from 0.08 to 0.36 – Slope method in the range from 0.05 to 0.53 – SRS method generally in the range from 0.15 to 0.85. Based on D_{utp} against σ'_v and D_{stp} against σ'_v plots, the curves of Taylor, Sridharan and Hyperbolic were lay above those of the Slope, Casagrande, and SRS indicated that the most similar values of time and settlement at EOP to those entrenched on the pore water pressure were obtained using the SRS method.

References

[1] G. Mesri, "Primary compression and secondary compression", in *Proceedings of the Symposium on Soil Behavior and Soft Ground Construction, 5–6 October 2001, Cambridge, USA*. American Society of Civil Engineers, 2001, pp. 122–166.

[2] G. Mesri and Y.K. Choi, "The uniqueness of the end-of-primary (EOP) void ratio-effective stress relationship", in *Proceedings of the eleven International Conference on Soil Mechanics and Foundation Engineering, 12–16 August 1985, San Francisco, USA*. A.A. Balkema, 1985, pp. 587–590.

[3] G. Grimstad, S.A. Degago, S. Nordal, and M. Karstunen, "Modeling creep and rate effects in structured anisotropic soft clays", *Acta Geotechnica*, vol. 5, no. 1, pp. 69–81, 2010, doi: 10.1007/s11440-010-0119-y.

[4] K. Terzaghi and O.K. Fröhlich, *Theorie der Setzung von Tonschichte*. Vienna, AT: Franz Deuticka, 1936.

[5] I. Smith, *Smith's Elements of Soil Mechanics*, 10th ed. Chichester: John Wiley & Sons, 2021.

[6] C.C. Ladd, R. Foott, K. Ishihara, F. Schlosser, and H.G. Poulos, "Stress-deformation and strength characteristics", in *Proceedings of the ninth International Conference on Soil Mechanics and Foundation Engineering, 10–15 July 1977, Tokyo, Japan*. Japanese Society of Soil Mechanics and Foundation Engineering, 1977, pp. 421–494.

[7] G. Mesri and Y.K. Choi, "Settlement analysis of embankments on soft clays", *Journal of the Geotechnical Engineering Division ASCE*, vol. 111, no. 4, pp. 441–464, 1985, doi: 10.1061/(ASCE)0733-9410(1985)111:4(441).

[8] S. Leroueil, M. Kabbaj, F. Tavenas, and R. Bouchard, "Stress-strain-strain rate relation for the sensitive natural clays", *Géotechnique*, vol. 35, no. 2, pp. 159–180, 1985, doi: 10.1680/geot.1985.35.2.159.

[9] S.A. Degago, G. Grimstad, H.P. Jostad, S. Nordal, and M. Olsson, "Use and miuse of the isotache concept with respect to creep hypotheses A and B", *Géotechnique*, vol. 61, no. 10, pp. 897–908, 2011, doi: 10.1680/geot.9.P.112.

[10] N. Oszczypko, The Miocene development of the Polish Carpathian Foredeep", *Przegląd Geologiczny*, vol. 49, no. 8, pp. 717–723, 2001.

[11] R. Kaczyński, "Wytrzymałość i odkształcalność górnomioceńskich iłów zapadliska przedkarpackiego", *Biuletyn Geologiczny Uniwersytetu Warszawskiego*, vol. 29, pp. 105–200, 1981.

[12] S. Kozłowski and Z. Kozydra, "Study on the marine clay deposits of the miocene in the carpathian fore-deep", *Przegląd Geologiczny*, vol. 13, no. 6, pp. 263–266, 1965.

[13] Z. Glazer and P. Dobak, "Estimation of value of general compressibility oedometric modulus on the basis of studies involving constant rate of deformation", *Przegląd Geologiczny*, vol. 27, no. 11, pp. 618–624, 1979.

[14] R. Kaczyński and J. Muchowski, "Mass movements on the slopes composed of the krakowiec clays (Exemplified in the Vistula and San valleys)", *Geological Quarterly*, vol. 31, no. 2/3, pp. 405–420, 1987.

[15] R. Pająk and P. Dobak, "Permeability parameters of Krakowiec clays evaluated in Rowe's consolidometer tests", *Geologia*, vol. 34, no. 4, pp. 677–689, 2008.

[16] K. Wilk, "Analysis of compressibility of layered Krakowiec Clays", *Przegląd Geologiczny*, vol. 62, no. 5, pp. 250–256, 2014.

[17] B. Olek, P. Dobak, and G. Gaszyńska-Freiwald, "Sensitivity evaluation of Krakowiec clay based on time-dependent behavior", *Open Geosciences*, vol. 10, no. 1, pp. 718–725, 2018, doi: 10.1515/geo-2018-0057.

[18] P.W. Rowe and L. Barden, "A new consolidation cell", *Géotechnique*, vol. 16, no. 2, pp. 162–170, 1966, doi: 10.1680/geot.1966.16.2.162.

[19] K.H. Head, *Manual of Soil Laboratory Testing: Effective Stress Tests*, 3rd ed. Caithness, Whittles Publishing, 2014.

[20] Y.K. Choi, "Consolidation behaviour of natural clays", PhD thesis, University of Illinois, 1982.

[21] G. Imai and Y.X. Tang, "Constitutive equation of one-dimensional consolidation derived from interconnected tests", *Soils and Foundations*, vol. 32, no. 2, pp. 83–6, 1992, doi: 10.3208/sandf1972.32.2_83.

[22] G. Mesri, "Primary and secondary compression", in *Soil Behavior and Soft Ground Construction*, J.T. Germaine, et al., Eds. ASCE, 2003, pp. 122–166, doi: 10.1061/40659(2003)5.

[23] T.W. Feng, "Compressibility and permeability of natural soft clays and surcharging to reduce settlements", PhD thesis, University of Illinois, 1991.

[24] M. Kabbaj, F. Tavenas, and S. Leroueil, "In situ and laboratory stress-strain relationships", *Géotechnique*, vol. 38, no. 1, pp. 83–100, 1988, doi: 10.1680/geot.1988.38.1.83.

[25] Y.T. Kim and S. Leroueil, "Modeling the viscoplastic behaviour of clays during consolidation: application to Berthierville clay in botch laboratory and field conditions", *Canadian Geotechnical Journal*, vol. 38, no. 3, pp. 484–497, 2001, doi: 10.1139/t00-108.

[26] P.A. Konovalov and S.G. Bezvolev, "Analysis of results of consolidation tests of saturated clayey soils", *Soil Mechanics and Foundation Engineering*, vol. 42, pp. 81–85, 2005, doi: 10.1007/s11204-005-0029-4.

[27] Y. Watabe, K. Udaka, and Y. Morikawa, "Strain rate effect on long-term consolidation of Osaka Bay clay", *Soils and Foundations*, vol. 48, no. 4, pp. 495–509, 2008, doi: 10.3208/sandf.48.495.

[28] J. Lowe and T.C. Johnson, "Use of back pressure to increase degree of saturation of test specimens", in *Proceedings of the Research Conference on Shear Strength of Cohesive Soils*. American Society of Civil Engineers, 1960, pp. 819–836.

[29] A. Casagrande and R.E. Fadum, *Notes on soil testing for engineering purposes. Harvard Soil Mechanics Series, No. 8*. Cambridge, Massachusetts, USA, 1940.

[30] D.W. Taylor, *Fundamentals of Soil Mechanics*. New York: Wiley, 1948.

[31] A. Sridharan and K. Prakash, "δ–t/δ method for the determination of coefficient of consolidation", *Geotechnical Testing Journal*, 1993, vol. 16 no. 1, pp. 131–134, doi: 10.1520/GTJ10276J.

[32] A. Sridharan and K. Prakash "Improved rectangular hyperbola method for the determination of coefficient of consolidation", *Geotechnical Testing Journal*, 1985, vol. 8, no. 1, pp. 37–40, doi: 10.1520/GTJ10855J.

[33] A. Sridharan, N.S. Murthy, and K. Prakash, "Rectangular hyperbola method of consolidation analysis", *Géotechnique*, vol. 37, no. 3, pp. 355–368, 1987, doi: 10.1680/geot.1987.37.3.355.

[34] S.K. Tewatia, "Evaluation of true cv and instantaneous cv, and isolation of secondary consolidation", *Geotechnical Testing Journal*, vol. 21, no. 2, pp. 102–108, 1998, doi: 10.1520/GTJ10748J.

[35] M.S. Al-Zoubi, "Coefficient of consolidation by the slope method", *Geotechnical Testing Journal*, vol. 31, no. 6, pp. 526–530, 2008, doi: 10.1520/GTJ100810.

[36] M.S. Al-Zoubi, "Consolidation analysis by the modified slope method", *Geotechnical Testing Journal*, vol. 37, no. 3, pp. 1–8, 2014, doi: 10.1520/GTJ20130097.

[37] M.S. Al-Zoubi, "Consolidation analysis using the settlement rate-settlement (SRS) method", *Applied Clay Science*, vol. 50, no. 1, pp. 34–40, 2010, doi: 10.1016/j.clay.2010.06.020.

[38] G. Mesri and Y.K. Choi "Discussion of Excess porewater pressure and preconsolidation effect developed in normally consolidated clays of some age", *Soils and Foundations*, vol. 20, no. 4, pp. 131–136, 1980.

[39] B.S. Olek, "Some remarks on the pore water pressure dissipation patterns from the one-dimensional consolidation test", *Archives of Civil Engineering*, vol. 68, no. 4, pp. 147–162, 2022, doi: 10.24425/ace.2022.143031.

[40] L.L. Zeng and Z.S. Hong, "Experimental study of primary consolidation time for structured and destructured clays", *Applied Clay Science*, vol. 116–117, pp. 141–149, 2015, doi: 10.1016/j.clay.2015.08.027.

[41] L.L. Zeng, S.S. Hong, and J. Han, "Experimental investigations on discrepancy in consolidation degrees with deformation and pore pressure variations of natural clays", *Applied Clay Science*, vol. 152, pp. 38–43, 2018, doi: 10.1016/j.clay.2017.10.029.

Wyznaczanie parametrów końca konsolidacji pierwotnej nad podstawie osiadań i nadciśnienia wody w porach

Słowa kluczowe: filtracja, ił, konsolidacja, koniec konsolidacji pierwotnej, nadciśnienie wody w porach

Streszczenie:

Z praktycznego punktu widzenia osiadanie grubych warstw gruntu w terenie przewiduje się w oparciu o ekstrapolację wyników badań laboratoryjnych przeprowadzonych na cienkich próbkach. W tym celu wykorzystuje się modelowe prawo konsolidacji, czyli „regułę H^2". Jej zastosowanie umożliwia w prosty sposób określenie zaawansowanie procesu konsolidacji w warstwie, pod warunkiem przyjęcia upraszczającego założenia, że zarejestrowane osiadania w badaniu konsolidacji wynikają wyłącznie z konsolidacji pierwotnej (rozpraszania nadciśnienia wody w porach). W artykule przedstawiono i przedyskutowano wyniki badań konsolidacji przeprowadzonych w konsolidometrze typu Bardena-Rowe na dwóch wysokoplastycznych iłach o przemodelowanej strukturze. Jako kryterium końca konsolidacji pierwotnej

(EOP) przyjęto jeden procent początkowej wartości nadciśnienia wody w porach. Na podstawie pomiarów osiadania w czasie przeanalizowano sześć metod wyznaczania czasu i osiadania (odkształcenia) na końcu konsolidacji pierwotnej. Dla wszystkich rozważanych krzywych konsolidacji pierwotny czas konsolidacji wyznaczony na podstawie zapisu osiadań próbki był zawsze mniejszy od czasu określonego poprzez obserwację nadciśnienia wody w porach. We wszystkich analizowanych przypadkach zaobserwowano brak całkowitego rozproszenia na końcu konsolidacji pierwotnej, określonego na podstawie osiadań. Wielkość pozostałego ciśnienia porowego w czasie na końcu konsolidacji pierwotnej określona różnymi metodami oraz stopień dodatkowego osiadania wywołanego pozostałym ciśnieniem porowym w czasie na końcu konsolidacji pierwotnej wskazały na niedoszacowanie parametrów EOP, gdy interpretacja badania opiera się wyłącznie na analizie pionowej deformacji próbki. W oparciu o średni stopień konsolidacji wynikający z rozproszenia nadciśnienia wody w porach w czasie na końcu konsolidacji pierwotnej uzyskano wartości czasu najbardziej zbliżone w EOP do ustalonych na podstawie kryterium rozproszenia nadmiernego ciśnienia wody porowej, stosując metody SRS, Casagrande i Slope. Obliczony stosunek czasu na końcu konsolidacji pierwotnej określony podczas analizy krzywej osiadania do czasu, gdy nadciśnienie wody w porach uznano za zakończone, zmieniał się wraz ze wzrostem pionowego naprężenia efektywnego i wskazywał na istnienie nierozproszonego ciśnienia porowego dla czasu EOP, bez względu na zastosowaną metodę interpretacji. Ogólnie najwyższe wartości stosunku obliczono dla najniższych wartości obciążenia, przy czym zaobserwowano wyraźną tendencję wzrostową wartości stosunku w następującej kolejności: metoda Taylora przeważnie w przedziale od 0,04 do 0,27 – metoda Sridharana przeważnie w przedziale od 0,04 do 0,27 – metoda Hiperboli prostokątnej przeważnie w przedziale od 0,04 do 0,34 – metoda Casagrande przeważnie w przedziale od 0,08 do 0,36 – metoda Nachylenia przeważnie w przedziale od 0,05 do 0,53 – metoda SRS przeważnie w przedziale od 0,15 do 0,85.